

# TRANSONIC HELICOPTER NOISE

A. S. Morgans <sup>\*</sup>, S. A. Karabasov <sup>†</sup>, A. P. Dowling <sup>‡</sup> and T. P. Hynes <sup>§</sup>  
*Department of Engineering, University of Cambridge, UK*

One of the most important issues facing the helicopter industry today is helicopter noise, of which transonic rotor noise is a major component. With the aim of obtaining a transonic rotor noise prediction method which is sufficiently fast to be useful to blade designers, this paper considers the Ffowcs Williams-Hawkings (FW-H) equation applied to a permeable control surface. The surface is chosen to be as small as possible while enclosing both the blade and any transonic flow regions. This allows the problematic quadrupole term in the FW-H equation to be neglected and requires only near field CFD computations. It is therefore less computationally time consuming than existing prediction methods and also offers insight into the physical origins of the noise. Noise predictions for transonic rotor blades in hover and forward flight are presented which show good agreement with experimental results, thus validating the methodology. Low order models for the dynamics of the acoustic sources are then derived for two-dimensional transonic flow. These are used to demonstrate that low order modelling techniques can be used to replace the need for full CFD solutions, providing significant time savings.

## Nomenclature

$A$	$= J \nabla_y f / \nabla_\eta f $	$\rho$	density, $kgm^{-3}$
$c$	speed of sound in undisturbed fluid, $ms^{-1}$	$\tau$	source time, $s$
$f$	$f = 0$ defines location of $S$	$\tau^*$	retarded time $= t - r(\tau^*)/c$ , $s$
$g$	$= t - \tau - r(\tau)/c$	$\phi$	phase, <i>radians</i>
$J$	Jacobian of $\mathbf{y} \rightarrow \eta$ coordinate change	$\psi$	blade azimuth angle, <i>degrees</i>
$L_i$	$= p_{ij}n_j + \rho u_i(u_n - v_n)$	$\bar{\omega}$	frequency, <i>rad/s</i>
$M$	Mach number	$(\ )$	generalised variable
$\mathbf{n}$	unit vector normal to $S$	$(\ )_0$	value in undisturbed fluid
$p$	absolute pressure, $Pa$	$(\ )'$	fluctuation about undisturbed/mean level
$p_{ij}$	compressive stress tensor, $Pa$	$(\ )_r$	component in radiation direction
$\mathbf{r}(\tau)$	$=  \mathbf{x}(t) - \mathbf{y}(\tau) $ , radiation vector, $m$	$(\ )_n$	component in surface normal direction
$r(\tau)$	$=  \mathbf{r}(\tau) $ , magnitude of $\mathbf{r}$ , $m$	$\square^2$	wave operator $= \nabla^2 - \frac{1}{c^2} \frac{\partial^2}{\partial t^2}$
$R$	blade tip radius, $m$		
$S$	control surface		
$t$	observer time, $s$		
$T$	sampling period, $s$		
$T_{ij}$	Lighthill stress tensor		
$\mathbf{u}$	fluid velocity, $ms^{-1}$		
$U_i$	$= (1 - \rho/\rho_0)v_i + \rho/\rho_0u_i$		
$\mathbf{v}$	velocity of $S$ , $ms^{-1}$		
$v$	speed of $S$ /blade speed (2-D flow), $ms^{-1}$		
$\mathbf{x}$	observer location, $m$		
$\mathbf{y}$	source location, $m$		
$z$	z-transform variable $= e^{i\omega T}$		
$\alpha$	blade pitch angle, <i>degrees</i>		
$\eta$	coordinates in which $S$ is stationary		

## Introduction

In recent years, factors such as environmental acceptability of ground noise levels, passenger comfort and acoustic detectability have elevated the importance of noise in helicopter rotor design. At present cruise speeds, shock associated rotor noise is a major noise source and yet there is presently no method of predicting it which is sufficiently fast and physically insightful to be useful in the rotor design process.

Rotor noise is most efficiently predicted using integral methods which separate the computation of the noise sources and noise propagation. The aerodynamic field around the blade is evaluated using an unsteady CFD solver, and an integral formulation is used to describe how the sound propagates to the far-field. The two most commonly used integral methods are the Kirchhoff method and Ffowcs Williams - Hawkings (FW-H) equation. The Kirchhoff method involves integration over a surface located in the linear flow region. Although it is capable of accurate noise prediction, the linear flow region is difficult to locate and is typically far from the blade for transonic flows.<sup>1,2</sup>

<sup>\*</sup>Graduate Student, asm28@eng.cam.ac.uk

<sup>†</sup>Post-doctoral Research Associate, sak36@eng.cam.ac.uk

<sup>‡</sup>Professor and Head of the Division of Energy, Fluid Mechanics and Turbomachinery, apd1@eng.cam.ac.uk

<sup>§</sup>Lecturer, tph@eng.cam.ac.uk

Presented at the American Helicopter Society 59th Annual Forum, Phoenix, Arizona, May 6-8 2003. Copyright © 2003 by the American Helicopter Society International, Inc. All rights reserved

Computing an accurate and well-resolved flow solution out to this surface therefore renders the Kirchhoff method too computationally intensive to be useful in design.<sup>3,4</sup> It also does not offer any physical insight into the noise generation. The FW-H equation expresses the noise in terms of a distribution of monopole and dipole sources over a control surface, and a distribution of quadrupole sources over the volume outside the surface.<sup>1</sup> When the control surface is chosen to coincide with the blade surface, these terms represent the noise due to blade thickness, blade loading and flow non-linearities/entropy variations respectively. The volume quadrupole term is difficult and time consuming to compute, but its contribution to the total noise is negligible except where the flow is transonic;<sup>5</sup> in these regions it may contribute significantly.

To predict shock-associated noise while avoiding the need to compute the problematic quadrupole term, the FW-H equation can be applied to a permeable control surface which encloses the blade and all transonic flow regions. The flow outside of the control surface is then subsonic and the quadrupole term can be neglected, leaving only the more straightforward surface source terms. The permeable form of the FW-H equation has recently been used to predict transonic helicopter noise,<sup>3,6</sup> but Kirchhoff-type control surfaces were used which were far from the blade. In terms of CFD computational time, this is far from optimal.

This paper considers a control surface which is as close to the blade surface as possible, while enclosing all transonic flow regions. With this arrangement, the quadrupole term in the FW-H equation can still be neglected, and yet the CFD solution requires significantly less computational time. The terms in the FW-H equation still offer physical insight into noise generation in terms of mass and momentum flux through the surface (for low tip Mach numbers, the control surface collapses onto the blade surface and the terms can be interpreted as before). This paper presents noise predictions for transonic three dimensional helicopter blade motion using the permeable surface form of the FW-H equation. The computational effort associated with these predictions is much less than would be required by the Kirchhoff method.

The control surface acoustic sources in the FW-H equation can always be calculated directly using unsteady CFD methods. However, in three-dimensions this will render any noise prediction method too time consuming for use in design for all but the most straightforward of manoeuvres. Low order modelling provides an efficient means of approximating the dynamics of the control surface acoustic sources. Full CFD computations under just a few conditions are needed, and these, combined with information on the time variation of the flight dynamics, allow the temporal variation of the acoustic sources to be predicted. Low order modelling essentially makes an efficient approxima-

tion to the CFD system.

For transonic flows such as those around a helicopter blade, the steady state flow-field is inherently a non-linear function of flight condition. However, the aim of low order modelling is to describe the dynamics of the unsteady flow field, which may behave as a linear perturbation about its quasi-steady value for sufficiently small variations in flight condition.<sup>7,8</sup>

This paper uses input/output modelling techniques appropriate for linear systems to obtain low order models for the dynamics of the control surface acoustic sources in two-dimensional transonic flow, and verifies that these models can replace the role of full CFD simulations in noise prediction.

### The Permeable Surface Form of the FW-H Equation

The permeable surface form of the Ffowcs Williams-Hawkings equation follows from the fluid conservation laws in the same way as the more familiar impermeable surface form.<sup>1</sup>

A permeable control surface,  $S$ , is considered which is defined by the equation  $f(\mathbf{x}, t) = 0$ .  $S$  encloses all solid boundaries and moves with velocity  $\mathbf{v}$ .

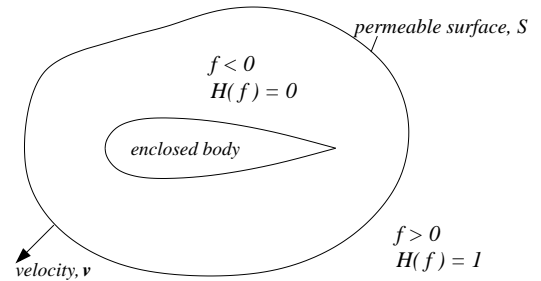


Fig. 1 Permeable control surface

Generalised flow variables are defined (denoted by an overbar) which hold over infinite space. Outside the surface,  $S$ , the generalised variables are equal to the real flow variables, while inside the surface they have the value zero. The continuity and momentum equations valid over all space can then be written as,

$$\frac{\partial \bar{\rho}'}{\partial t} + \frac{\partial (\bar{\rho} u_i)}{\partial x_i} = (\rho_0 u_n + \rho'(u_n - v_n)) \delta(f) |\nabla_{\mathbf{x}} f| \quad (1)$$

$$\frac{\partial (\bar{\rho} u_i)}{\partial t} + \frac{\partial}{\partial x_j} (\bar{p}_{ij} + \bar{\rho} u_i u_j) = (\bar{p}_{ij} n_j + \bar{\rho} u_i (u_n - v_n)) \delta(f) |\nabla_{\mathbf{x}} f| \quad (2)$$

Following the notation of di Francescantonio,<sup>6</sup> new variables,  $U_i$  and  $L_i$  are introduced to simplify the algebra. These represent velocity and stress tensors, modified to account for the flow through  $S$ .

$$\begin{aligned} L_i &= \bar{p}_{ij} n_j + \bar{\rho} u_i (u_n - v_n) & (L_m &= L_i M_i) \\ U_i &= (1 - \rho/\rho_0) v_i + \rho/\rho_0 u_i \end{aligned} \quad (3)$$

By subtracting the divergence of (2) from the time derivative of (1), an inhomogeneous wave equation is obtained.

$$\begin{aligned} \square^2 p'(\mathbf{x}, t) = & -\frac{\partial}{\partial x_i} (L_i \delta(f) |\nabla_{\mathbf{x}} f|) \\ & + \frac{\partial}{\partial t} (\rho_0 U_n \delta(f) |\nabla_{\mathbf{x}} f|) + \frac{\partial^2 \overline{T}_{ij}}{\partial x_i \partial x_j} \end{aligned} \quad (4)$$

This is the differential form of the FW-H equation and describes the generation and propagation of sound. On the right hand side, surface monopole, surface dipole and volume quadrupole distributions act as acoustic sources, while on the left the wave operator describes the propagation of sound from the sources to the observer. The substitution  $p' = c^2 \rho'$  has been made on the left side of the equation, requiring linearity and no entropy variation at the observer location.  $\overline{T}_{ij}$  is the generalised Lighthill stress tensor, which has value  $T_{ij} = \rho u_i u_j + p_{ij} - c^2 \rho' \delta_{ij}$  outside of the surface  $S$  and is zero within it. Since  $S$  encloses the blade and all transonic flow regions,  $T_{ij}$  is negligible outside of  $S$  and hence the last term on the right hand side can be neglected.

The equation is valid in all of three dimensional space, owing to the fact that generalised variables have been used. The integral form can therefore be obtained by convolving with the free space, 3-D Green's function for the wave equation, which has the well known form  $\delta(t - |\mathbf{x}|/c)/(4\pi|\mathbf{x}|)$ .<sup>9</sup>

$$\begin{aligned} p'(\mathbf{x}, t) = & -\frac{\partial}{\partial x_i} \int_{-\infty}^{+\infty} \frac{L_i \delta(f) \delta(g) |\nabla_{\mathbf{y}} f|}{4\pi r} d^3 \mathbf{y} d\tau \\ & + \frac{\partial}{\partial t} \int_{-\infty}^{+\infty} \frac{\rho_0 U_n \delta(f) \delta(g) |\nabla_{\mathbf{y}} f|}{4\pi r} d^3 \mathbf{y} d\tau \end{aligned} \quad (5)$$

$$\text{where } r = |\mathbf{x} - \mathbf{y}(\tau)| \quad \text{and } g = t - \tau - r/c$$

A coordinate change from fixed coordinates,  $\mathbf{y}$ , to coordinates which move with the control surface,  $\eta$ , allows the source strengths to be considered in a frame moving with the surface. The Jacobian for the coordinate change is  $J$ , and represents the ratio of volume elements in the  $\eta$  and  $\mathbf{y}$  spaces.

$$\begin{aligned} p'(\mathbf{x}, t) = & -\frac{\partial}{\partial x_i} \int_{-\infty}^{+\infty} \frac{L_i \delta(f) \delta(g) |\nabla_{\mathbf{y}} f| J}{4\pi r} d^3 \eta d\tau \\ & + \frac{\partial}{\partial t} \int_{-\infty}^{+\infty} \frac{\rho_0 U_n \delta(f) \delta(g) |\nabla_{\mathbf{y}} f| J}{4\pi r} d^3 \eta d\tau \end{aligned} \quad (6)$$

Equation (6) is the most general integral form of the permeable FW-H equation. To implement it numerically, it is necessary to integrate the two delta functions. The retarded

time formulation provides a convenient means of doing this in cases where the motion of the surface  $S$  is subsonic. Firstly integration over  $\tau$  is performed: since the surface  $S$  is fixed in  $\eta$  coordinates, the  $\delta(f)$  term is unaffected by this. Noting that  $|\partial g / \partial \tau| = |1 - M_r|$  and integrating over one space dimension using the remaining delta function gives,

$$\begin{aligned} p'(\mathbf{x}, t) = & -\frac{\partial}{\partial x_i} \int_S \left[ \frac{L_i A}{4\pi r |1 - M_r|} \right]_{\tau^*} dS(\eta) \\ & + \frac{\partial}{\partial t} \int_S \left[ \frac{\rho_0 U_n A}{4\pi r |1 - M_r|} \right]_{\tau^*} dS(\eta) \end{aligned} \quad (7)$$

Equation (7) is the permeable surface form of the retarded time formulation with the quadrupole term neglected.  $A = J |\nabla_{\mathbf{y}} f| / |\nabla_{\eta} f|$  represents the ratio of area elements in the  $\eta$  and  $\mathbf{y}$  spaces. If the surface is undistorted in motion then  $A$  is equal to unity.  $\tau^*$  is the retarded time, given implicitly by the relationship,

$$\tau^* = t - \frac{r(\tau^*)}{c} = t - \frac{|\mathbf{x}(t) - \mathbf{y}(\tau^*)|}{c} \quad (8)$$

Sound emitted by the source at retarded time  $\tau^*$  will reach the observer at the time of interest,  $t$ . For a fixed observer position and time and for subsonic surface motion,  $\tau^*$  can only have one value.

To express equation (7) in a form suitable for computation, further manipulation is required. Numerical differentiation of the integrals can be avoided and the speed and accuracy of the computation is improved if the derivatives are taken inside the integrals.<sup>10</sup> The  $\partial / \partial x_i$  can be replaced using (9) and the integration surface  $S(\eta)$  is independent of  $t$  so time derivatives inside the integrals can be replaced with  $\partial / \partial \tau$  terms using (10).

$$\frac{\partial}{\partial x_i} \int_S Q_i dS = \frac{\partial}{\partial t} \int_S \frac{Q_i r_i}{cr} dS + \int_S \frac{Q_i r_i}{r^2} dS \quad (9)$$

$$\frac{\partial [Q(\tau)]_{\tau^*}}{\partial t} = \left[ \frac{1}{(1 - M_r)} \frac{\partial Q(\tau)}{\partial \tau} \right]_{\tau^*} \quad (10)$$

Differentiating and gathering terms together gives,

$$\begin{aligned} 4\pi p'(\mathbf{x}, t) = & \int_S \left[ \frac{\rho_0 (\dot{U}_n + U_{\dot{n}})}{r(1 - M_r)^2} \right]_{\tau^*} dS(\eta) + \\ & \int_S \left[ \frac{\rho_0 U_n (r(\partial \mathbf{M} / \partial \tau)_r + c(M_r - |\mathbf{M}|^2))}{r^2(1 - M_r)^3} \right]_{\tau^*} dS(\eta) \\ & + \frac{1}{c} \int_S \left[ \frac{\dot{L}_r}{r(1 - M_r)^2} \right]_{\tau^*} dS(\eta) \\ & + \int_S \left[ \frac{L_r - L_m}{r^2(1 - M_r)^2} \right]_{\tau^*} dS(\eta) + \\ & \frac{1}{c} \int_S \left[ \frac{L_r (r(\partial \mathbf{M} / \partial \tau)_r + c(M_r - |\mathbf{M}|^2))}{r^2(1 - M_r)^3} \right]_{\tau^*} dS(\eta) \end{aligned} \quad (11)$$

Equation (11) is the form of the impermeable retarded time formulation that has been used for numerical computation. It is valid for subsonic surface motion and it assumes that the integration surface is undistorted in motion, so that  $A = 1$  and  $\partial A / \partial \tau = 0$ .

### CFD Methodology

The primary interest here is in shock-associated noise. Typically, the shock is present over the outer part of the span for azimuthal angles corresponding to the blade advancing. For this phase of the cycle, the interaction with other blade wakes and the disturbance due to the presence of the fuselage and tail rotor are likely to be small. The CFD calculation used to generate the data for the acoustic calculations is therefore performed for a single, oscillating and advancing blade in an otherwise undisturbed flow.

The calculations are performed using a grid which is *fixed relative to the blade*, with the problem formulated in terms of the relative velocity as in Zhong and Qin.<sup>11</sup> This makes it relatively easy to form smooth acoustic surfaces and to ensure good grid and solution quality in their vicinity. In addition, it removes errors introduced by the need to re-interpolate the solution at each time step onto a new grid position that one has if a pitching grid technique<sup>12</sup> is used.

Although the blade is treated as a rigid body, this approach has been used successfully to account for a wide range of blade motion, such as collective and cyclic pitch variation, tilt and coning. Non-inertial terms due to the highly convoluted motion of the blade frame appear as volumetric sources in this formulation. It is important to handle these terms in a manner which is compatible with the conservative nature of the discretisation scheme for the equations of motion and with the non-reflective nature of the boundary conditions. Provided this is done, however, no extra complication appears to arise from using this accelerating frame approach.<sup>13</sup>

The governing equations were discretised in a control volume fashion by assembling numerical fluxes across interfaces using well-proven shock-capturing methods. The explicit characteristic Roe scheme was implemented together with Van Leer's variable extrapolation (MUSCL) of 2nd/3rd order in characteristic variables in each grid direction. Unwanted numerical oscillations were minimised using the Total Variation Diminishing approach, which was applied to limit the slopes of the characteristic variables using the MinMod limiter. Slight modifications were made to the standard MUSCL TVD variable extrapolation formulae to account for non-uniform grid spacing.

The solid-wall rotor blade boundary conditions were applied by assembling the outer fluxes and eliminating the velocity component normal to the wall. In order to reduce the entropy generation near the solid boundary more accurate estimates for fluxes adjacent to the boundary were

made by the introduction of symmetric fictitious points lying inside the blade surface.

At the outer boundary, a range of non-reflecting boundary conditions were used to judge the domain size necessary to ensure that the solution at the acoustic surfaces was unaffected by the boundary presence.

The computational grid consisted of a series of chord-wise O-type grids stacked in the blade span-wise direction. At the blade tip the grid was wrapped around forming a hemispherical blade cap to provide a uniform mesh distribution away from the blade. A modification of the flux assembling procedure was needed for where the confluence of the blade cap radial lines and the blade grid met to ensure that the algorithm remained uniform and conservative. This grid strategy proved to be quite robust in application to a number of rectangular blade geometries.

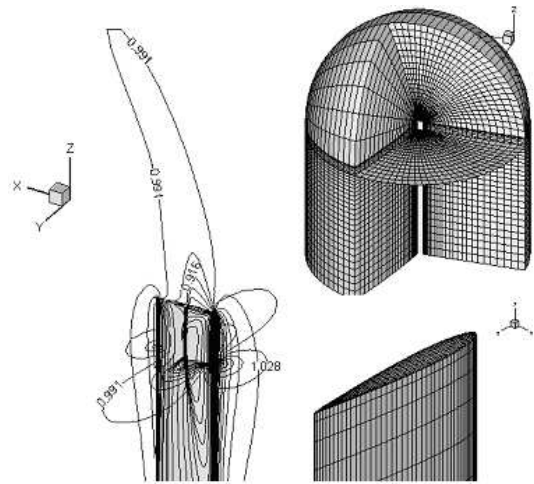


**Fig. 2 Computational grid and pressure field around a hovering UH-1H rotor blade at  $M_H=0.88$**

The inviscid solver was tested in a number of one and two-dimensional initial value problems.<sup>14,15</sup> A simplified but effective way of applying non-reflecting boundary conditions was also developed and tested on a number of problems involving a 2-D transonic pitching blade section accelerating and decelerating in the free stream.<sup>16</sup>

The three-dimensional Euler solver has been validated against several hover and forward flight benchmarks and has been shown to give good agreement of the calculated blade surface/near-field pressure variations with experiments and other calculations. For example, figure 3 shows the near-field comparison for a two-blade rotor at  $M_T = 0.7634$  and  $\mu = 0.25$  at the  $r/R = 0.88$  blade station in forward flight.<sup>17</sup>

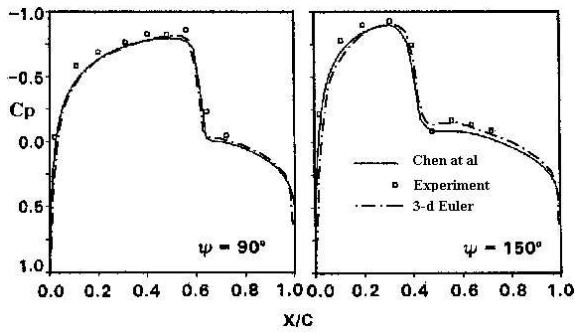


Fig. 3 Forward flight simulation

### Noise Prediction Results

Computations of the aerodynamic field generated by a rotating helicopter blade were performed for hover and forward flight. The flow in the vicinity of the blade was transonic for at least part of the rotational cycle, although tip Mach numbers were sufficiently low to avoid shock delocalisation. The CFD method was used to calculate the aerodynamic field around the blade and the permeable surface form of the FW-H equation was used to generate noise predictions.

### Hover

An isolated UH-1H blade with an aspect ratio of 13.7 was considered in non-lifting hover; an advantage of non-lifting blades is that wake-blade interaction complications are avoided. Noise calculations were performed at two different tip Mach numbers, 0.85 and 0.88, both of which involved a supersonic flow pocket above the outer part of the blade. The noise at an observer lying in the rotor plane a distance of 3.09 rotor radii from the axis of rotation was calculated by applying the FW-H equation to four different control surfaces, all of which enclosed the outer part of the blade and supersonic flow regions.

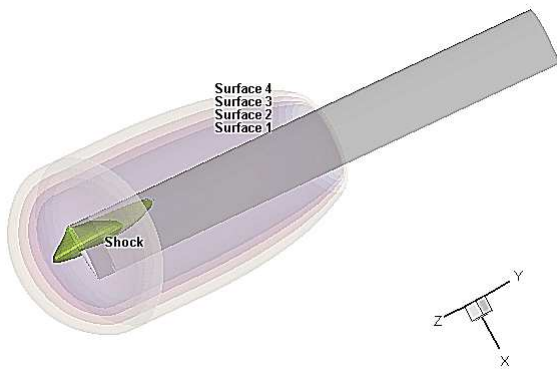


Fig. 4 The four permeable control surfaces to which the FW-H was applied

Since the blade motion was periodic, the noise at the observer was also periodic. It had the form of a large negative pressure peak preceded and followed by a much smaller

positive pressure peak, the characteristic signature of rotor plane shock-associated noise. For both rotor tip Mach numbers, applying the FW-H equation to any of the four control surfaces gave very similar results. This was to be expected as the difference in noise prediction from adjacent surfaces is equal to the noise generated by the quadrupole sources in the volume between them. The surfaces have been chosen such that these volumes consist of entirely subsonic flow and hence this should be negligible. The difference between the further out adjacent surfaces is likely to be due to numerical noise rather than physical quadrupole sources; the ratio of the real solution to numerical noise decreases with distance from the blade as the real pressure field becomes weaker and grid coarsening causes numerical viscosity and domain boundary effects to increase.

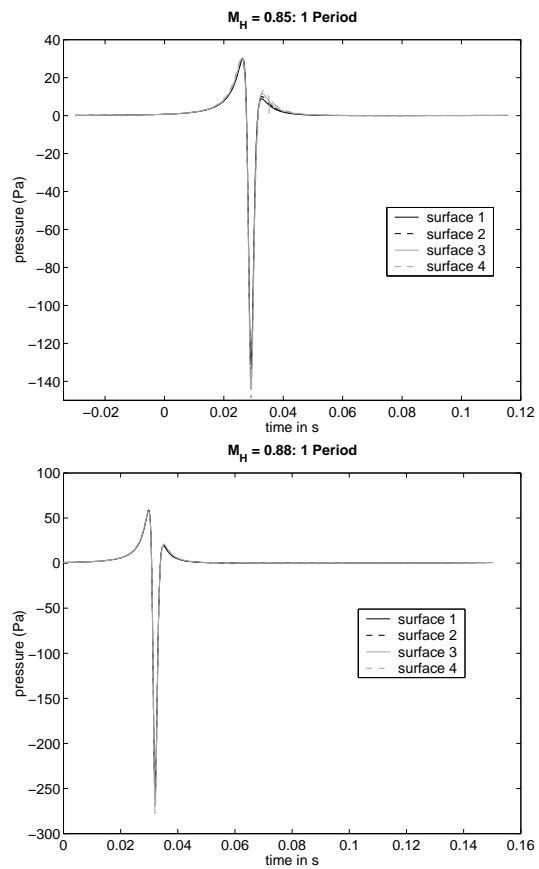
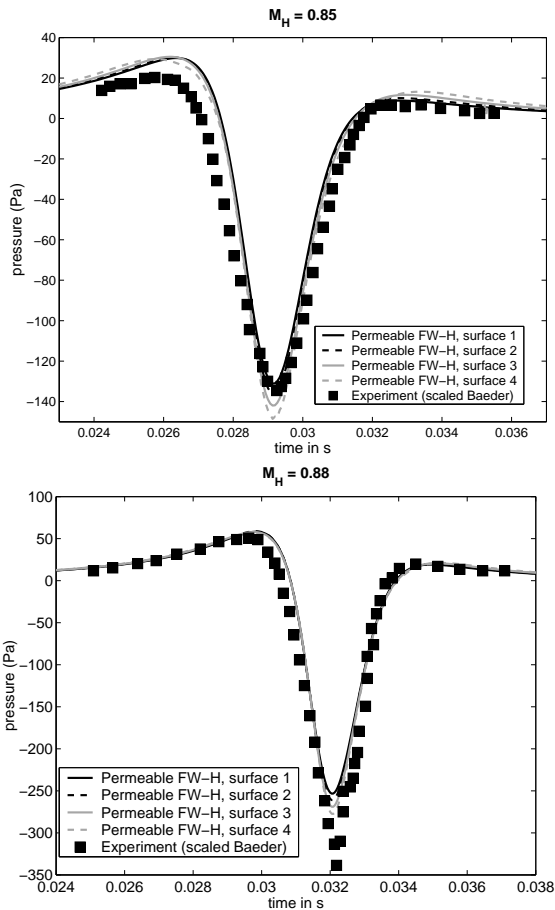


Fig. 5 Predicted sound at an observer in the rotor plane,  $r_{obs}/R_{tip}=3.09$ , for a non-lifting UH-1H blade in hover

Experimental noise measurements in the vicinity of the negative pressure peaks exist<sup>18</sup> and by enlarging the scale of the graphs in around the negative pressure peak, as in figure 6, it is seen that the noise predictions compare well with them. The experimental results were for a 1/7th scale blade model and so the time axis has been scaled to correspond to a full-size blade.



**Fig. 6 Comparison between predictions and experiment of the predicted sound at an observer in the rotor plane,  $r_{obs}/R_{tip}=3.09$ , for non-lifting UH-1H blade in hover**

### Forward Flight

The noise prediction method was now applied to the more challenging problem of forward flight. A rectangular OLS blade with an aspect ratio of 9.22 was considered in forward flight with a hover tip Mach number of 0.664, an advance ratio 0.2605 and an advancing tip Mach number 0.837; the blade was once again non-lifting.

Unlike in the hover test cases, a supersonic flow pocket no longer existed throughout the rotational cycle of the blade. It was now restricted to between azimuth angles of approximately  $\psi = 70^\circ$  and  $\psi = 135^\circ$ , using the convention of  $\psi = 90^\circ$  and  $\psi = 270^\circ$  being the advancing and retreating positions respectively. The strongest shock occurred at  $\psi = 105^\circ$  and the Mach contours for this position are shown in figure 7.

The sound at three observer positions was calculated using the permeable surface form of the FW-H equation. Three control surfaces were used which enclosed the supersonic region when at its largest. All observers were in the plane of the rotor and translated with the rotor axis such

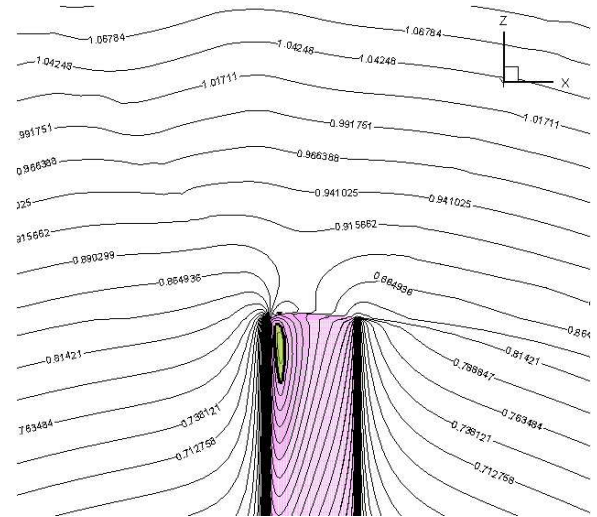


**Fig. 7 Mach contours around the upper blade surface at  $\psi=105^\circ$  for an OLS blade in forward flight**

that the distance between the axis and the observers was fixed at  $r/R = 3.44$ . The angle between the observer and the downstream direction was varied as shown in figure 8. Noise prediction results compared to some experimental measurements<sup>19</sup> are shown in figure 9.

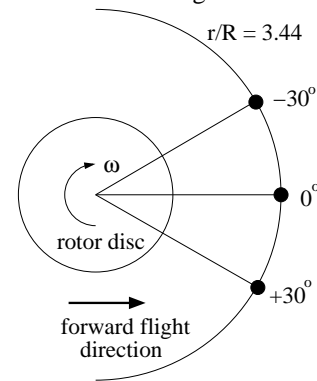


**Fig. 8 The observer locations in the frame of the rotation axis**

For all three observer positions, a negative pressure peak was immediately preceded and followed by a smaller positive peak. The predictions from the three different control surfaces were in close agreement, the difference again being due to the physical or numerical quadrupole sources contained in the volume between them. The predicted wave shapes and peak magnitudes are in excellent agreement with those from experiment, and the noise variation with blade azimuth angle is similar. The small shift in the azimuth response is probably due to a slightly lower advance ratio (0.258) being used in the experiments: there is some ambiguity in the Baeder paper<sup>19</sup> as to the advance ratio / advancing tip Mach number combination that has been used. For both the predicted and experimental results, the peak response occurs somewhere between  $-30^\circ$  and

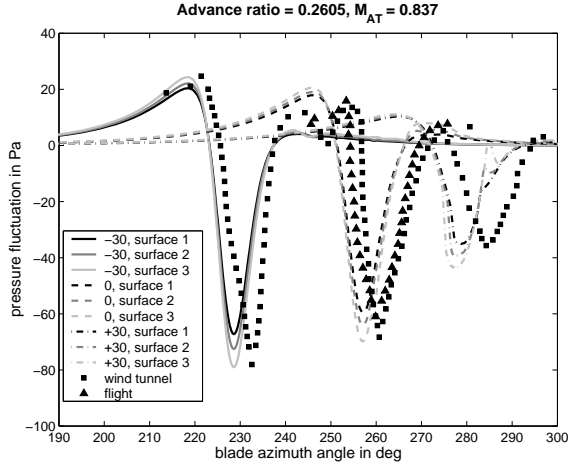


**Fig. 9** Sound predictions in the rotor plane for 3 observers at  $r/R = 3.44$  for a non-lifting rectangular OLS blade in forward flight

$0^\circ$ , corresponding to a location upstream of the advancing rotor blade.

Although the availability of experimental data has limited test cases to non-lifting blades, the noise prediction method is able to predict the noise due to lifting blades incorporating variable pitch, coning and rotor disc tilt.

### Low Order Modelling

In the previous section, the values of the flow variables on the control surface were calculated using an unsteady CFD method. While this is feasible for hover and steady forward flight, in more complicated helicopter manoeuvres the associated computational effort will be restrictive.

A more efficient alternative is to approximate the dynamics of the flow quantities relevant to noise prediction using low order models. In this case, the relevant flow quantities are the “acoustic sources” on the control surface, given by  $\rho_0 U_n$  and the vector  $L_i$  in equation (7). By developing low order models to describe the dynamics of  $\rho_0 U_n$  and  $L_i$  in response to flight condition variations, an unsteady CFD computation is needed only for a few time steps rather than for the full simulation.

In general, low order models for  $\rho_0 U_n$  and  $L_i$  are required at all grid points on the three-dimensional control surface. To demonstrate the principles of low order modelling without this quantity of information, two-dimensional flow has been considered so that the section of the control surface can be taken as constant and only the variation of acoustic sources along the contour of the section need be considered.

If the retarded time variations across a given section are small (the surface section is compact) then the acoustic sources combine in equation (7) as straightforward contour integrals multiplied by their associated length. The surface section will be compact if the  $M_r$  term is sufficiently small.

Thus under the conditions of two-dimensional flow and a compact surface section, low order models to describe the dynamics of the following integrals:

$$\int_C \rho_0 U_n dC, \quad \int_C L_x dC, \quad \int_C L_y dC \quad (12)$$

, where  $C$  is the contour of the control surface section, provide sufficient information for noise prediction. By obtaining low order models for the above acoustic source integrals, the technique and power of low order modelling can be neatly demonstrated.

In two-dimensional flow, the flight condition variables are blade speed and blade pitch angle. These are taken to be the system inputs with the system outputs being the acoustic source integrals in equation (12). It was initially assumed (and later shown) that the system exhibited dynamic linearity, meaning that input and output variations about their mean or quasi-steady values were linearly related. Dynamic linearity enables system identification to be used to develop low order models.

System identification is an input/output modelling technique for developing a mathematical model of a dynamic system using observed system data.<sup>20</sup> It fits the parameters of a model structure to measured input and output data and its success depends on the choice of model structure and the quantity and quality of data used. It has recently been used in approximating unsteady CFD solutions around complex bodies<sup>21</sup> and in approximating flame transfer functions in combustion oscillations.<sup>22</sup>

An important issue in system identification is the form of the input signals, in this case the blade speed and blade pitch angle variations. Input signals must have a numerically practical form, have a sufficiently large frequency bandwidth and should not be susceptible to significant noise contamination. Ljung<sup>20</sup> and Zhu et al<sup>22</sup> have evaluated the suitability of different forms of input signal for CFD simulations and concluded that a “sum of sines” input signal is an appropriate choice. The “sum of sines” signal for a single-input system has the form,

$$f'(t) = \hat{f} \sum_{k=1}^K \sin(\omega_k t + 2\pi\phi_k) \quad (13)$$

where  $K$  is the number of sinusoids spread equally over the passband,  $\omega_k = \omega_{min} + (k-1)(\omega_{max} - \omega_{min})/(K-1)$ ,  $k = 1 \dots K$  and  $\omega_{min}$  and  $\omega_{max}$  are the lower and upper limits of the passband. To ensure that the component sinusoids are independent, the phase of the  $k$ th sinusoid at  $t = 0$  is  $2\pi\phi_k$  where  $\phi_k$  is a random number chosen from a uniform distribution on the interval  $(0, 1)$ .  $\hat{f}$  is simply a scaling constant.

For a multi-input system, each input signal is made up of a “sum of sines” as in the single input case, but the frequencies contained in each signal interlace one another over the passband. For the two-input system under consideration,

the blade speed and blade pitch angle inputs had the following form:

$$v(t) = 262.2 + 0.6 \sum_{k=1}^{170} \sin(\omega_k t + 2\pi\phi_k)$$

$$\alpha(t) = 3.66 + 0.08 \sum_{j=1}^{170} \sin(\omega_j t + 2\pi\phi_j) \quad (14)$$

where  $\omega_k = 6 + 2(k-1)$ ,  $\omega_j = 4 + 2(j-1)$

The mean levels of 262.2 m/s and 3.66 degrees were chosen so that the flow above the blade surface would always be transonic i.e. there would always be a shock present. Preliminary studies of the shock dynamics had suggested that shock emergence and disappearance is a non-linear regime which is not well modelled using system identification. Interest was therefore confined to the regime described as type A shock motion by Tijdeman;<sup>23</sup> the shock strengths are largest in this regime and so it is likely to be the main regime of interest in terms of shock-noise generation. As is standard for dynamically linear systems, the mean levels of the input and output signals were neglected when performing the system identification and just the fluctuating parts of the signals were used.

For the system identification, an IIR (infinite impulse response) filter model structure was used. For a given input, this represents the corresponding output as a linear combination of previous outputs and present and previous inputs. For a single-input single-output (SISO) system the equation is,

$$o'(t) = \sum_{i=0}^I a_i f'(t-iT) + \sum_{j=1}^J b_j o'(t-jT) \quad (15)$$

Taking  $z$ -transforms gives:

$$o'(z) = \frac{\sum_{i=0}^I a_i z^{-i}}{1 - \sum_{j=1}^J b_j z^{-j}} f'(z) \quad (16)$$

For larger numbers of inputs or outputs, the  $z$ -transform method of expressing the IIR filter structure is more suitable. For the two-input system being considered, the IIR filter structure used was:

$$o'(z) = \frac{\sum_{i=0}^I a_i z^{-i}}{1 - \sum_{j=1}^J b_j z^{-j}} f'_1(z) + \frac{\sum_{k=0}^K c_k z^{-k}}{1 - \sum_{l=1}^L d_l z^{-l}} f'_2(z) \quad (17)$$

where  $f'_1$ ,  $f'_2$  and  $o'$  are the inputs and output respectively,  $T$  is the sampling period,  $(I, J)$  and  $(K, L)$  are the filter orders and  $a_i$ ,  $b_j$ ,  $c_k$  and  $d_l$  are the constant coefficients. The process of system identification aims to find the coefficients which give best fit to the data, in this case obtained from the CFD simulation.

## Results

The dynamic response of the acoustic source integrals, as measured from the CFD simulation and as predicted by the IIR filter model structure are shown in figure 10.

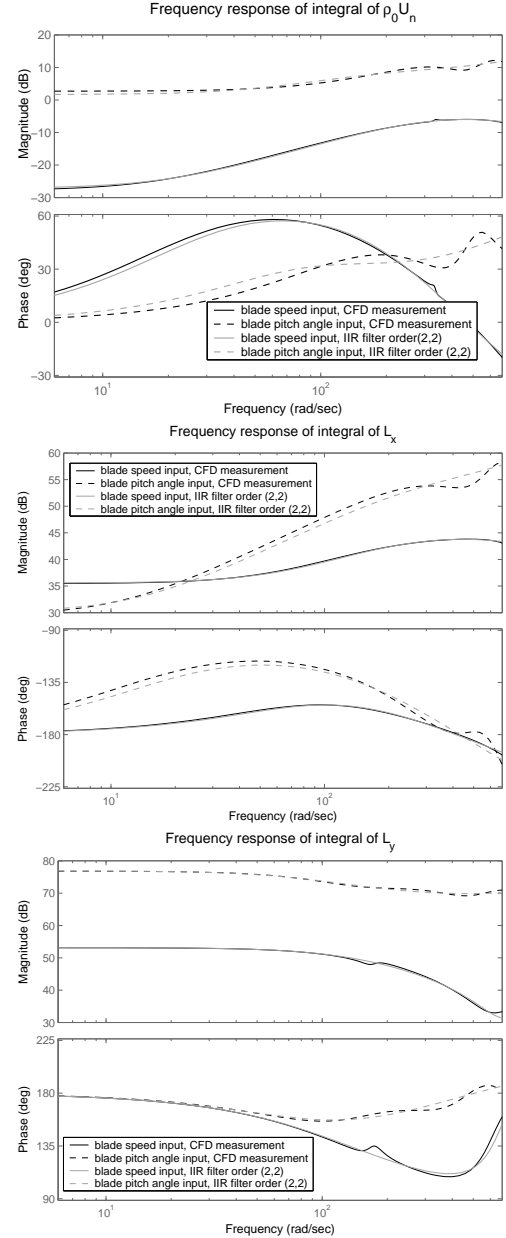


**Fig. 10** The frequency response of the acoustic source integrals in response to blade speed and blade pitch angle variations

It is seen that filters of order (2,2) are sufficient to approximate the dynamics accurately. This means that information at just four initial times (two if one of the inputs is zero) is required to predict all subsequent behaviour, although it should be noted that the sampling period used in system identification is larger than the CFD time step.

The exact form of the filters is shown below where  $I_1 = \int_C \rho_0 U_n dC$ ,  $I_2 = \int_C L_x dC$  and  $I_3 = \int_C L_y dC$ .

$$I_1'(z) = \frac{0.0850 - 0.130z^{-1} + 0.0452z^{-2}}{1 - 1.92z^{-1} + 0.921z^{-2}} v'(z) + \frac{53.4 - 103z^{-1} + 49.7z^{-2}}{1 - 0.806z^{-1} - 0.180z^{-2}} \alpha'(z) \quad (18)$$

$$I_2'(z) = \frac{-44.3 + 73.0z^{-1} - 28.8z^{-2}}{1 - 1.90z^{-1} + 0.899z^{-2}} v'(z) + \frac{17000 - 35200z^{-1} + 18200z^{-2}}{1 - 0.0139z^{-1} - 0.939z^{-2}} \alpha'(z) \quad (19)$$

$$I_3'(z) = \frac{-135 + 266z^{-1} - 131z^{-2}}{1 - 1.90z^{-1} + 0.898z^{-2}} v'(z) + \frac{-5540 - 10500z^{-1} - 4960z^{-2}}{1 - 1.81z^{-1} + 0.813z^{-2}} \alpha'(z) \quad (20)$$

The frequency response for each of the inputs varying in isolation was also found by holding the other constant at its mean level. In both cases, the same response as in figure 10 was found, validating the assumption of dynamic linearity.

As mentioned previously, the integrals of the acoustic source integrals can be used in sound prediction if the flow is two-dimensional and sufficiently subsonic. Such a case was considered, involving an infinitely long blade of constant cross section. The blade pitch angle was held constant at 3.66 degrees and the blade speed varied sinusoidally as  $v(t) = 262.2 + 15.6\cos(100t)$ . The sound originating from the central 1m length was considered at an observer whose position was fixed in the frame of the blade. The observer location was chosen so that the maximum value of  $M_r$  at any point on the permeable control surface was 0.6, which is sufficiently low to justify the assumption of compactness.

The sound at the observer location as a function of time was then calculated using the permeable surface form of the FW-H equation in three different ways.

1. By calculating the retarded time at each point on the control surface and using full CFD data.
2. By assuming constant retarded time across the section of the control surface and using full CFD data.
3. By assuming constant retarded time across the surface section and using low order models for the acoustic source integrals instead of CFD data.

The agreement between the first two is a measure of how compact the surface section is; the agreement between the latter two is a measure of how well the low order models are performing. It can be seen from figure 11 that all three are in close agreement, confirming that low order models are able to replace the need for a full CFD simulation. The actual behaviour of the acoustic source integrals throughout

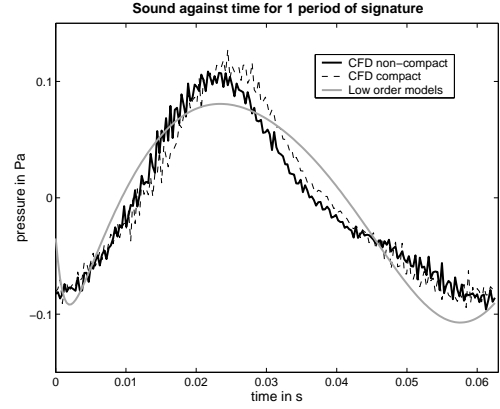


**Fig. 11 Comparison of sound prediction using CFD and low order models**

the cycle compared to that predicted by the low order models is shown in figure 12. It should be noted that this level of accuracy is achieved with filters of order just (2, 2); by increasing the filter orders the accuracy could be improved still further.

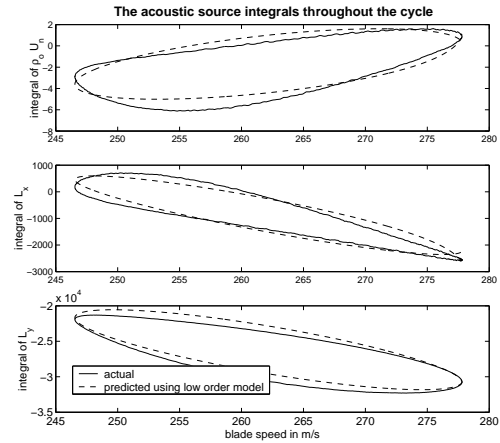


**Fig. 12 The behaviour of the acoustic source integrals throughout the blade speed cycle**

The above has demonstrated that low order models can be used to replace the need for a full CFD simulation in two-dimensional flow. The methodology would be much the same for three dimensional flow, the only difference being that models for the acoustic sources  $\rho_0 U_n$ ,  $L_x$ ,  $L_y$  and  $L_z$  would need to be derived for those points on the control surface which contributed significantly to the integrals.

## Conclusions

The permeable form of the FW-H equation has been used to predict transonic rotor noise with much less computational effort than has previously been possible. The methodology involved applying the FW-H equation to control surfaces which were very small while enclosing both the blade and all transonic flow regions. Such a choice of

control surface allowed the quadrupole term in the FW-H equation to be neglected and meant that an accurate CFD solution was required only in the vicinity of the blade. This methodology also allowed some physical insight into the noise generation to be retained.

Noise predictions for both hover and forward flight test cases were obtained by using an Euler based CFD method to calculate the flow variables on the control surface. The permeable surface form of the FW-H equation (the retarded time formulation with the quadrupole term neglected) was then used to calculate the propagation of sound from the control surface to the observer. The noise predictions showed very good agreement with experimental results, validating the methodology.

It was then demonstrated that low order modelling techniques can be used to approximate the effect of changing flight conditions on those flow variables relevant to noise generation. The implications of this are that low order models can replace the need for a full unsteady CFD calculation in cases where this would be too time consuming, such as for three-dimensional manoeuvres. For ease of illustration, two-dimensional transonic flow for which the control surface section was acoustically compact was considered. Low order models for the section contour integrals of the acoustic sources were obtained using system identification techniques appropriate for dynamically linear systems. The low order models were used in noise prediction and the results were in close agreement to those obtained using a full CFD simulation.

### Acknowledgments

The authors are grateful to the Engineering and Physical Sciences Research Council (EPSRC), Westland Helicopters Ltd and Thales Underwater Systems Ltd for their financial support.

### References

- <sup>1</sup>Williams, J. E. F. and Hawkins, D. L., "Sound Generation by Turbulence and Surfaces in Arbitrary Motion," *Philosophical Transactions of the Royal Society*, Vol. A264, 1969, pp. 321–342.
- <sup>2</sup>Lyrantzis, A. and Xue, Y., "Versatile Kirchhoff Code for Aeroacoustic Predictions," *AIAA Journal*, Vol. 35, No. 1, 1997.
- <sup>3</sup>Brentner, K. S. and Farassat, F., "Analytical Comparison of the Acoustic Analogy and Kirchhoff Formulation for Moving Surfaces," *AIAA Journal*, Vol. 36, No. 8, 1998, pp. 1379–1386.
- <sup>4</sup>Brentner, K. S., Lyrantzis, A. S., and Koutsavdis, E. K., "Comparison of Computational Aeroacoustic Prediction Methods for Transonic Rotor Noise," *Journal of Aircraft*, Vol. 34, No. 4, 1997, pp. 531–538.
- <sup>5</sup>Hanson, D. B. and Fink, M. R., "The Importance of Quadrupole Sources in Prediction of Transonic Tip Speed Propeller Noise," *Journal of Sound and Vibration*, Vol. 62, No. 1, 1979, pp. 19–38.
- <sup>6</sup>di Francescantonio, P., "A New Boundary Integral Formulation for the Prediction of Sound Radiation," *Journal of Sound and Vibration*, Vol. 202, No. 4, 1997, pp. 491–509.
- <sup>7</sup>Dowell, E. H., Hall, K. C., and Romanowski, M. C., "Reduced Order Aerodynamic Modeling of How to Make CFD Useful to an Aeroelastician," *ASME Aerospace Division*, Vol. 53-3, No. 149-163, 1997.
- <sup>8</sup>Ballaus, W. F. and Goorjian, P. M., "Computation of Unsteady Transonic Flows by Indicial Methods," *AIAA Journal*, Vol. 16, No. 2, 1978, pp. 117–124.
- <sup>9</sup>Crighton, D. G., Dowling, A. P., Williams, J. E. F., Heckl, M., and Leppington, F. G., *Modern Methods in Analytical Acoustics*, Springer-Verlag, 1992.
- <sup>10</sup>Farassat, F. and Succi, G. P., "The Prediction of Helicopter Rotor Discrete Frequency Noise," *Vertica*, Vol. 7, No. 4, 1983, pp. 309–320.
- <sup>11</sup>Zhong, B. and Qin, N., "Non-Inertial Multiblock Navier-Stokes Calculation for Hovering Rotor Flow Fields Using Relative Velocity Approach," *The Aeronautical Journal*, July 2001, pp. 379–389.
- <sup>12</sup>Shaw, S. T. and Qin, N., "Unsteady Flow Around Helicopter Blade Sections in Forward Flight," *The Aeronautical Journal of the Royal Aeronautical Society*, 1999.
- <sup>13</sup>Karabasov, S. A. and Hynes, T. P., "A Perturbed Non-Linear Euler Method for Calculations in Non-Inertial Frames of Reference," In preparation.
- <sup>14</sup>Karabasov, S. A., Hynes, T. P., and Goloviznin, V. M., "Comparative Analysis of Several High-Resolution TVD Schemes for the One-Dimensional Euler Equations," *Finite Difference Scheme Conference*, Palanga, Lithuania, 2000.
- <sup>15</sup>Karabasov, S. A. and Hynes, T. P., "Unsteady Calculation of 2-D Inviscid Flow with Shocks," *The 6th International Conference MMA*, Vilnius, Lithuania, 2001.
- <sup>16</sup>Karabasov, S. A. and Hynes, T. P., "Open Boundary Conditions of Predictor - Corrector Type for External Flows," *8th AIAA/CEAS Aeroacoustics Conference*, No. 2002-2442, Breckenridge, CO, USA, June 2002.
- <sup>17</sup>Chen, C. L., McCroskey, W. J., and Obayashi, S., "Numerical Solutions of Forward-Flight Rotor Flow Using an Upwind Method," *Journal of Aircraft*, Vol. 28, 1991, pp. 374–380.
- <sup>18</sup>Baeder, J. D., Gallman, J. M., and Yu, Y. H., "A Computational Study of the Aeroacoustics of Rotor in Hover," *Journal of the American Helicopter Society*, Vol. 42, No. 1, 1997, pp. 39–53.
- <sup>19</sup>Baeder, J. D., "Euler Solutions to Nonlinear Acoustics of Non-Lifting Rotor Blades," *International Technical Specialists Meeting at Rotorcraft Acoustics and Rotor Fluid Dynamics*, Philadelphia, PA, USA, October 1991.
- <sup>20</sup>Ljung, L., *System Identification: Theory for the User*, chap. 1, Prentice-Hall, 1987.
- <sup>21</sup>Cowan, T. J., Jr., A. S. A., and Gupta, K. K., "Accelerating Computational Fluid Dynamics Based Aeroelastic Predictions Using System Identification," *Journal of Aircraft*, Vol. 38, No. 1, 2001, pp. 81–87.
- <sup>22</sup>Zhu, M., Dowling, A. P., and Bray, K. N. C., "Flame Transfer Function Calculations for Combustion Oscillations," *ASME International Gas Turbine and Aeroengine Congress and Exhibition*, No. 2001-FT-374, New Orleans, June 2001.
- <sup>23</sup>Tijdeman, H. and Seebass, R., *Annual Review of Fluid Mechanics*, chap. Transonic Flow Past Oscillating Airfoils, 1980, pp. 181–222.